

Geochemical evidence for widespread euxinia in the Later Cambrian ocean

Benjamin C. Gill¹†, Timothy W. Lyons¹, Seth A. Young², Lee R. Kump³, Andrew H. Knoll⁴ & Matthew R. Saltzman⁵

Widespread anoxia in the ocean is frequently invoked as a primary driver of mass extinction as well as a long-term inhibitor of evolutionary radiation on early Earth. In recent biogeochemical studies it has been hypothesized that oxygen deficiency was widespread in subsurface water masses of later Cambrian oceans^{1,2}, possibly influencing evolutionary events during this time^{1–3}. Physical evidence of widespread anoxia in Cambrian oceans has remained elusive and thus its potential relationship to the palaeontological record remains largely unexplored. Here we present sulphur isotope records from six globally distributed stratigraphic sections of later Cambrian marine rocks (about 499 million years old). We find a positive sulphur isotope excursion in phase with the Steptoean Positive Carbon Isotope Excursion (SPICE), a large and rapid excursion in the marine carbon isotope record, which is thought to be indicative of a global carbon cycle perturbation^{4,5}. Numerical box modelling of the paired carbon sulphur isotope data indicates that these isotope shifts reflect transient increases in the burial of organic carbon and pyrite sulphur in sediments deposited under large-scale anoxic and sulphidic (euxinic) conditions. Independently, molybdenum abundances in a coeval black shale point convincingly to the transient spread of anoxia. These results identify the SPICE interval as the best characterized ocean anoxic event in the pre-Mesozoic ocean and an extreme example of oxygen deficiency in the later Cambrian ocean. Thus, a redox structure similar to those in Proterozoic oceans^{6–8} may have persisted or returned in the oceans of the early Phanerozoic eon. Indeed, the environmental challenges presented by widespread anoxia may have been a prevalent if not dominant influence on animal evolution in Cambrian oceans.

Cambrian carbonates preserve large, rapid (of a few million years duration or less) and globally correlated excursions in the marine carbon isotope record ($\delta^{13}\text{C}_{\text{carb}}$), indicating perturbations in the global carbon cycle^{4,9–11}. The driving mechanisms behind these events, however, are poorly understood. What makes these excursions particularly interesting to geobiologists is that many of them coincide with biological events recorded by fossils, suggesting links between biological and environmental history^{3,4}. Here we focus on the last large excursion of the period, the SPICE.

The SPICE is recorded as a +4–6‰ shift in $\delta^{13}\text{C}_{\text{carb}}$ that occurs globally in later Cambrian successions (beginning of the Furongian International Series and Paibian International Stage, 499 million years ago); it is thought to have lasted 2–4 million years^{4,5}. A well-documented extinction of trilobites coincides with the onset of the SPICE on the palaeocontinent of Laurentia^{4,12}, and the isotopic excursion has also been correlated to intervals of biological turnover on other palaeocontinents¹³. The SPICE is also coincident with global changes in sea level; its onset coincides with a transgressive event, and its peak is concurrent with a lowstand recorded as the Sauk-II/III hiatus^{4,5}.

We report sulphur isotope data from six globally distributed stratigraphic sections across the SPICE event that reveal parallel, positive

carbon and sulphur isotope excursions (Figs 1, 2 and 3). These sections represent diverse sedimentary environments. Thus, similarities among the trends, despite differences in depositional conditions, indicate the global and primary nature of the geochemical signals (see Supplementary Information for details of individual stratigraphic sections and data supporting the preservation of the geochemical signals).

The SPICE sulphur isotope excursion is one of the largest identified in the geologic record and is the first to be correlated globally at a high scale of resolution. This excursion occurs in both carbonate-associated sulphate ($\delta^{34}\text{S}_{\text{CAS}}$) and pyrite ($\delta^{34}\text{S}_{\text{pyrite}}$), which further supports a primary marine signal, and its magnitude indicates a major perturbation in the global sulphur cycle. There are, however, significant differences in the details of the sulphate sulphur isotope trends among basins. In particular, the pre-event $\delta^{34}\text{S}_{\text{CAS}}$ baseline differs in the various locations (Fig. 2): some records show relatively steady sulphur isotope values before the excursion (that is, western and eastern Laurentia), but Gondwanan data show a positive trend up-section before the excursion proper (Fig. 2).

Furthermore, despite overarching similarities, the absolute values and amplitudes of the excursion also differ among the studied basins. The Gondwanan record is the most extreme, with $\delta^{34}\text{S}_{\text{CAS}}$ values reaching almost +70‰ and an amplitude of +35‰ (Fig. 2). On the other end of the spectrum, the record in eastern Laurentia shows a peak value of +38‰ and amplitude of only +12‰ (Fig. 2). Sulphate isotope data from the contemporaneous Port au Port Group from Newfoundland show little evidence of a sulphur isotope excursion during the SPICE event², but those results contain only a single data point near the peak of the SPICE. The $\delta^{34}\text{S}_{\text{CAS}}$ relationships at this locality need to be investigated further before conclusions can be drawn.

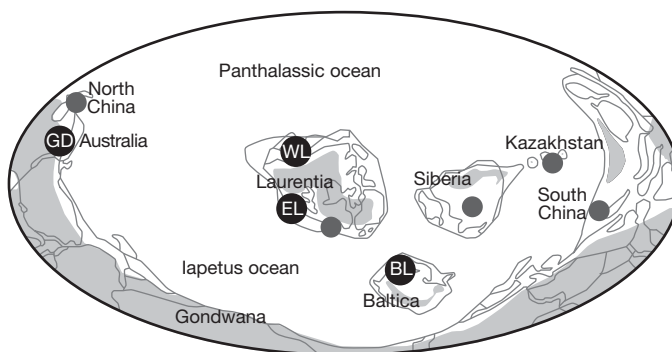


Figure 1 | Palaeo-reconstruction of the later Cambrian Earth. The reconstruction is based on ref. 27 and shows locations where the SPICE has been identified (filled circles). Locations investigated in this study are: Western Laurentia (WL) = Shingle Pass and Lawson Cove, Great Basin, USA; Eastern Laurentia (EL) = TE-1 Texas County Core, Missouri, USA; Gondwana (GD) = Mount Whelan no. 1 and Mount Murray, Queensland, Australia; Baltica (BL) = Andrarum no. 3 core, Sweden.

¹Department of Earth Sciences, University of California, 900 University Avenue, Riverside, California 92521, USA. ²Department of Geological Sciences, Indiana University-Bloomington, 1001 East 10th Street, Bloomington, Indiana 47405-1405, USA. ³Department of Geosciences, Penn State University, 503 Deike Building, University Park, Pennsylvania 16802, USA. ⁴Department of Organismic and Evolutionary Biology, Harvard University, 26 Oxford Street, Cambridge, Massachusetts 02138, USA. ⁵School of Earth Science, The Ohio State University, 275 Mendenhall Laboratory, 125 South Oval Mall, Columbus, Ohio 43210, USA. †Present address: Department of Earth and Planetary Sciences Harvard University, 20 Oxford Street, Cambridge, Massachusetts 02138, USA.

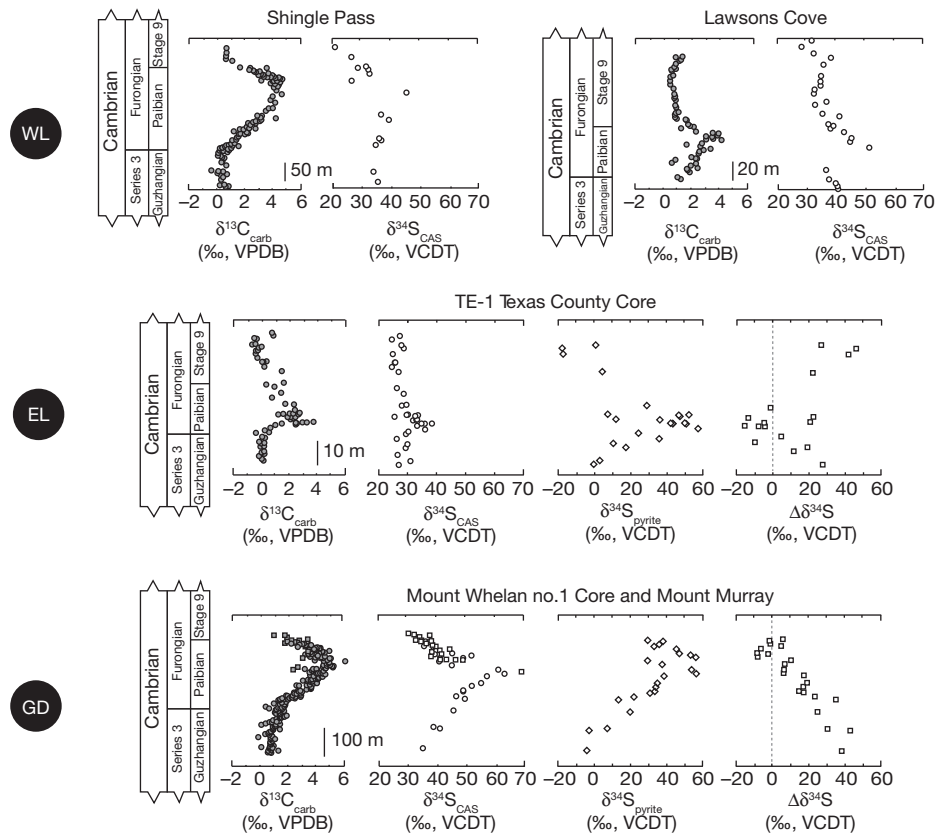


Figure 2 | Chemostratigraphies of the SPICE carbonate stratigraphic sections. Isotope data are plotted by stratigraphic height in metres. International series and stages are based on published biostratigraphy and the most recent definitions of the subdivisions for the Cambrian Period (see Supplementary Information). Carbon isotope profiles from Great Basin sections and Mount Whelan no. 1 core are from refs 10 and 4, respectively. CAS

sulphur isotope profile for Shingle Pass is from ref. 15. On the GD $\delta^{13}\text{C}_{\text{carb}}$ and $\delta^{34}\text{S}_{\text{CAS}}$ plots, circles are from Mount Whelan no. 1 Core and squares from the Mount Murray outcrop. Carbon and sulphur isotope data are reported as per mil (‰) deviations from the isotope composition of Vienna Pee Dee Belemnite (VPDB) and Vienna Cañon Diablo Troilite (VCDT), respectively.

Overall, these isotopic differences support the idea that the sulphur reservoir in the later Cambrian ocean was spatially heterogeneous and that sulphate concentrations were therefore low^{14,15}. We also observe that the sulphate isotope excursion peaks stratigraphically slightly before the carbon isotope maximum (see Supplementary Fig. 2), which suggests that the sulphate reservoir was relatively more sensitive to change than the marine pool of dissolved inorganic carbon. This state of sulphate in later Cambrian seawater differed greatly from the modern reservoir, which is relatively homogeneous globally with a concentration of 28 mmol kg^{-1} (mM) and a sulphur isotope composition of +21‰. This contrast with the modern value indicates that the residence time of sulphate in the Cambrian ocean was much less than today's.

The parallel behaviour between the carbon and sulphur isotope excursions (Fig. 2) suggests that the SPICE records a transient increase

in the amount of carbon and sulphur buried as organic matter and pyrite (FeS_2) in marine sediments. Such parallel burial occurs in anoxic marine sediments and beneath euxinic water columns¹⁶—that is, beneath water columns that are both anoxic and contain free hydrogen sulphide. Organic matter fuels microbial sulphate reduction, and pyrite is formed when H_2S produced from microbial sulphate reduction reacts with iron minerals and is buried along with the residual organic matter. Ultimately, the burial of both species results in the removal of carbon and sulphur from the ocean. This coupling can result in positive isotope shifts for both species in seawater: the carbon and sulphur leaving the ocean through burial are enriched in ^{12}C and ^{32}S via isotope fractionations accompanying photosynthetic and microbial sulphate reduction pathways, respectively, leaving the seawater correspondingly enriched in ^{13}C and ^{34}S .

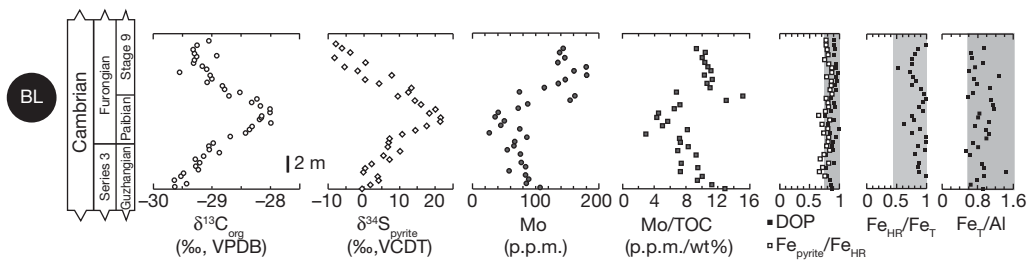


Figure 3 | Chemostratigraphy from the Andrarum no. 3 Core of the Alum Shale, Sweden (Baltica). The carbon isotope profile is from ref. 28. The shaded regions of the plots of degree of pyritization (DOP), $\text{Fe}_{\text{pyrite}}/\text{Fe}_{\text{HR}}$, $\text{Fe}_{\text{HR}}/\text{Fe}_{\text{T}}$ and $\text{Fe}_{\text{T}}/\text{Al}$ cover values that indicate anoxia and euxinia: $\text{Fe}_{\text{T}}/\text{Al}$ values appreciably above 0.5 and $\text{Fe}_{\text{HR}}/\text{Fe}_{\text{T}}$ above 0.4 indicate deposition under anoxic waters²⁹,

and DOP and $\text{Fe}_{\text{pyrite}}/\text{Fe}_{\text{HR}}$ values above 0.75 are conservatively diagnostic of euxinic environments³⁰. We note that the decrease and minimum in Mo and Mo/TOC correspond to the initiation and peak of the carbon and sulphur isotope excursions, respectively. C_{org} , organic carbon. TOC, total organic carbon. $\text{Fe}_{\text{pyrite}}$, pyrite iron. Fe_{HR} , highly reactive iron. Fe_{T} , total iron.

We tested this hypothesis by modelling the ocean inventories of carbon and sulphur during the SPICE. Specifically, we constructed a simple box model that simulates the cycling of each element in the ocean (see Supplementary Information for details). The model shows that the isotope excursions can be replicated by transiently increasing the amount of organic carbon buried by factors of 1.5 to 2.5 and pyrite sulphur by factors of 2.5 to 4.5 for a duration of 0.5 to 1.5 million years (Fig. 4, and see Supplementary Information for additional model details).

Importantly, our model puts quantitative constraints on the size of the marine sulphate reservoir during the later Cambrian period. An assumption of pre-SPICE sulphate concentrations greater than 2.5 mM demands more than 8 million years for recovery of $\delta^{34}\text{S}_{\text{sulphate}}$ (that is, return to the pre-event baseline) following the SPICE (Supplementary Fig. 9), which is unreasonable in light of the available constraints on SPICE duration⁵. Our simulations suggest, therefore, that the concentration of seawater sulphate was very low—at or below the low end of the 2–12 mM range suggested by previous work^{14,15}.

Another important result from the model is that the predicted ratio of carbon to sulphur (C/S) linked to this transient burial was very low: 1 to 4 moles of C per mole of S or 0.4–1.5 grams of C per gram of S (Fig. 4). In younger sediments, similar C/S ratios are observed only in sediments deposited under euxinic conditions¹⁶. The large scale of this Cambrian euxinia is suggested by comparison to the Black Sea, the largest modern euxinic basin. Our estimates for the transient burial flux of sulphur that caused the isotope excursion are equal to 50–75 times that of the euxinic portion of the Black Sea¹⁷, thus providing the first quantitative evidence for widespread euxinia in the Palaeozoic ocean. Importantly, these estimates do not come close to predicting whole-ocean euxinia and probably reflect pervasive sulphidic mid-water-column conditions along basin margins.

Our argument for increased euxinia becomes stronger when we consider that ΔS may have decreased over the event (Fig. 2). ΔS (now preserved as $\Delta\delta^{34}\text{C}_{\text{CAS-pyrite}}$) is the isotopic offset between coexisting

seawater sulphate (preserved as CAS) and dissolved hydrogen sulphide (preserved as pyrite) that results from microbial sulphate reduction and associated microbial pathways that lead to pyrite formation. For the two sections that have sufficient pyrite for isotopic analysis (eastern Laurentia and Gondwana), there is a strikingly systematic negative shift for ΔS parallel to the positive excursions for $\delta^{34}\text{S}_{\text{CAS}}$ and $\delta^{13}\text{C}_{\text{carb}}$ (Fig. 2). This shift is important because a smaller ΔS , when applied to our model, requires even greater pyrite burial to explain the positive sulphur excursion. The further increase in pyrite burial results in a lower mean C/S ratio, strengthening the case for burial under euxinic conditions (see Supplementary Fig. 12 for sensitivity tests of ΔS). Our Cambrian data must record a decrease in seawater sulphate concentration associated with progressive, voluminous euxinic pyrite burial during the SPICE under generally low levels of sulphate.

Additional evidence for the expansion of euxinic conditions comes from the coeval Alum Shale in Sweden, where a systematic decrease in Mo enrichment coincides with the SPICE (Fig. 3). Molybdenum is a transition metal typically enriched in organic-rich sediments deposited under euxinic conditions, with extents of enrichment tracking overall Mo availability in the local or global system as well as concentrations of organic carbon^{18,19}. The decreasing enrichment seen in the Alum Shale is also apparent when Mo concentrations are normalized to total organic carbon content, suggesting that organic content is not the primary control. Importantly, the variability in Mo concentrations and Mo/TOC ratios occur despite iron proxy data that point to persistent euxinia over the interval of interest (Fig. 3); the Alum basin appears to have been locally euxinic before, during and after the SPICE.

The suggestion then is that another process drove the scale of enrichment. In short, the decline going into the SPICE and increase coming out argue for a decrease in the global Mo inventory of seawater as euxinic conditions expanded and then contracted on a globally significant scale^{8,19,20}—a scenario consistent with the predictions of the modelled C and S data. We envision conditions during the SPICE to have been analogous to those during ocean anoxic events of the Mesozoic era, when the spread of euxinia led to extensive deposition of organic-rich, pyritic sediments in the deeper ocean, yielding concomitant isotopic shifts in dissolved inorganic carbon²¹ and seawater sulphate²².

The geochemical and stratigraphic framework of the SPICE provides new insight into the pronounced biological turnover associated with this event. Taken together with evidence for an initial sea-level rise, the geochemical data suggest that shoaling of toxic anoxic waters onto the shelf led to the extinction of shelf fauna, a situation similar to that envisioned for end-Permian extinctions²³. Such a scenario was proposed previously to explain recurrent later Cambrian trilobite extinctions¹² but in acknowledged absence of independent constraints for such conditions.

Additional oscillations observed in the later Cambrian marine $\delta^{13}\text{C}$ record could reflect environmental perturbations similar to those linked to the SPICE. We suggest that anoxic water masses occurred widely in the subsurface of the later Cambrian ocean (that is, below the wind-mixed surface layer), a view that finds qualitative support in the stratigraphic distribution of organic-rich, pyritic black shales that peak in abundance in later Cambrian successions²⁴. If correct, the high rates of biological turnover²⁵ and repeated trilobite extinctions^{12,26} documented for later Cambrian fossils can be at least partially explained by episodic expansion of oxygen-depleted waters. In larger terms, broad patterns of Cambrian animal evolution may reflect persistent oxygen deficiency in subsurface waters of Cambrian oceans, shedding new light on early evolution of the Phanerozoic biosphere in the wake of late Proterozoic oxygenation.

Received 21 June; accepted 16 November 2010.

- Hough, M. L. *et al.* A major sulphur isotope event at c. 510 Ma: a possible anoxia-extinction-volcanism connection during the Early–Middle Cambrian transition? *Terra Nova* **18**, 257–263 (2006).
- Hurtgen, M. T., Pruss, S. B. & Knoll, A. H. Evaluating the relationship between the carbon and sulfur cycles in the later Cambrian ocean: an example from the Port au

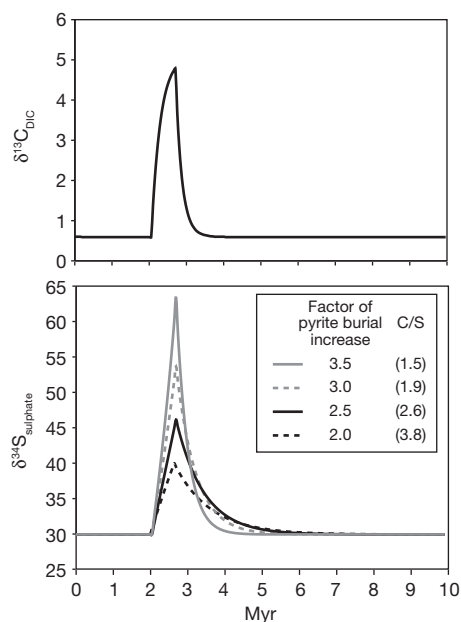


Figure 4 | Examples of the modelled carbon and sulphur isotope composition of the ocean during the SPICE. To generate the isotope excursions, we doubled organic carbon burial from 4.1×10^{18} to 8.2×10^{18} moles per million years and increased pyrite burial from the steady-state rate (0.98×10^{18} moles per million years) by the factors given for half a million years. Values in parentheses are the molar carbon-to-sulphur (C/S) ratio of the transient burial fluxes introduced into the model. The starting marine sulphate concentration in these simulations was 1.5 mM. DIC, dissolved inorganic carbon.

- Port Group, western Newfoundland, Canada. *Earth Planet. Sci. Lett.* **281**, 288–297 (2009).
3. Zhuravlev, A. & Wood, R. Anoxia as the cause of the mid-Early Cambrian (Botomian) extinction event. *Geology* **24**, 311–314 (1996).
 4. Saltzman, M. *et al.* A global carbon isotope excursion (SPICE) during the Late Cambrian: relation to trilobite extinctions, organic-matter burial and sea level. *Palaeogeogr. Palaeoclimatol. Palaeoecol.* **162**, 211–223 (2000).
 5. Saltzman, M. R. *et al.* The Late Cambrian SPICE ($\delta^{13}\text{C}$) Event and the Sauk II-SAUK III Regression: new evidence from Laurentian basins in Utah, Iowa and Newfoundland. *J. Sedim. Res.* **74**, 366–377 (2004).
 6. Canfield, D. E. A new model for Proterozoic ocean chemistry. *Nature* **396**, 450–453 (1998).
 7. Poulton, S. W., Fralick, P. W. & Canfield, D. E. The transition to a sulphidic ocean ~1.84 billion years ago. *Nature* **431**, 173–177 (2004).
 8. Scott, C. *et al.* Tracing the stepwise oxygenation of the Proterozoic ocean. *Nature* **452**, 456–459 (2008).
 9. Brasier, M. D., Corfield, R. M., Derry, L. A., Rozanov, A. Y. & Zhuravlev, A. Y. Multiple $\delta^{13}\text{C}$ excursions spanning the Cambrian explosion to the Botomian crisis in Siberia. *Geology* **22**, 455–458 (1994).
 10. Saltzman, M. R., Runnegar, B. & Lohmann, K. C. Carbon isotope stratigraphy of Upper Cambrian (Steptoean Stage) sequences of the eastern Great Basin: record of a global oceanographic event. *Geol. Soc. Am. Bull.* **110**, 285–297 (1998).
 11. Montañez, I. P., Osleger, D. A., Banner, J. L., Mack, L. E. & Musgrove, M. Evolution of the Sr and C isotope composition of Cambrian Oceans. *GSA Today* **10**, 1–7 (2000).
 12. Palmer, A. The biomere problem: evolution of an idea. *J. Paleontol.* **58**, 599–611 (1984).
 13. Peng, S. *et al.* Global standard stratotype—section and point of the Furongian series and Paibian stage Cambrian. *Lethaia* **37**, 365–379 (2004).
 14. Brennan, S. T., Lowenstein, T. K. & Horita, J. Seawater chemistry and the advent of biocalcification. *Geology* **32**, 473–476 (2004).
 15. Gill, B. C., Lyons, T. W. & Saltzman, M. R. Parallel, high-resolution carbon and sulfur isotope records of the evolving Paleozoic marine sulfur reservoir. *Palaeogeogr. Palaeoclimatol. Palaeoecol.* **256**, 156–173 (2007).
 16. Berner, R. Sedimentary pyrite formation: an update. *Geochim. Cosmochim. Acta* **48**, 605–615 (1984).
 17. Neretin, L. N., Volkov, I. I., Böttcher, M. E. & Grinenko, V. A. A sulfur budget for the Black Sea anoxic zone. *Deep Sea Res. I* **48**, 2569–2593 (2001).
 18. Emerson, S. & Huested, S. Ocean anoxia and the concentrations of molybdenum and vanadium in seawater. *Mar. Chem.* **34**, 177–196 (1991).
 19. Algeo, T. J. & Lyons, T. W. Mo–total organic carbon covariation in modern anoxic marine environments: Implications for analysis of paleoredox and paleohydrographic conditions. *Paleoceanography* **21**, PA1016 (2006).
 20. Algeo, T. J. Can marine anoxic events draw down the trace element inventory of seawater? *Geology* **32**, 1057–1060 (2004).
 21. Arthur, M. A., Dean, W. E. & Pratt, L. M. Geochemical and climatic effects of increased marine organic carbon burial at the Cenomanian/Turonian boundary. *Nature* **335**, 714–717 (1988).
 22. Adams, D. D., Hurtgen, M. T. & Sageman, B. B. Volcanic triggering of a biogeochemical cascade during Oceanic Anoxic Event 2. *Nature Geosci.* **3**, 1–4 (2010).
 23. Wignall, P. B. & Twitchett, R. J. Oceanic anoxia and the end Permian mass extinction. *Science* **272**, 1155–1158 (1996).
 24. Berry, W. B. N. & Wilde, P. Progressive ventilation of the oceans: an explanation for the distribution of the lower Paleozoic black shales. *Am. J. Sci.* **278**, 257–275 (1978).
 25. Bambach, R. K., Knoll, A. H. & Wang, S. C. Origination, extinction, and mass depletions of marine diversity. *Paleobiology* **30**, 522–542 (2004).
 26. Palmer, A. R. Biomere: a new kind of biostratigraphic unit. *J. Paleontol.* **39**, 149–153 (1965).
 27. Scotese, C. R. *Atlas of Earth History* (PALEOMAP Project, 2001).
 28. Ahlberg, P. *et al.* Cambrian high-resolution biostratigraphy and carbon isotope chemostratigraphy in Scania, Sweden: first record of the SPICE and DICE excursions in Scandinavia. *Lethaia* **42**, 2–16 (2008).
 29. Lyons, T. W. & Severmann, S. A critical look at iron paleoredox proxies: new insights from modern euxinic marine basins. *Geochim. Cosmochim. Acta* **70**, 5698–5722 (2006).
 30. Raiswell, R., Buckley, F., Berner, R. A. & Anderson, T. F. Degree of pyritization of iron as a paleoenvironmental indicator of bottom-water oxygenation. *J. Sedim. Res.* **58**, 812–819 (1988).

Supplementary Information is linked to the online version of the paper at www.nature.com/nature.

Acknowledgements NSF-EAR and NASA Astrobiology provided funding. Fieldwork and sample collection were aided by S. Bates, L. Bongers, H. Dayton, S. Mason, P. McGoldrick, J. Owens, C. Seeger and E. Starbuck. Sulphur isotope analyses were aided by S. Bates and W. Gilhooly. We thank P. Ahlberg and M. Eriksson for allowing access to the Andrarum no. 3 drill core. Discussions with G. Love, N. Hughes, D. Johnston, P. Cohen and T. Dahl improved the manuscript.

Author Contributions B.C.G., T.W.L., M.R.S. and S.A.Y. collected samples used in this study. B.C.G. did the chemical analyses and collected mass spectrometer and ICP-MS data. B.C.G. and L.R.K. built the geochemical box model. B.C.G. wrote the manuscript, with contributions from T.W.L., A.H.K. and L.R.K. All the authors contributed to discussions and interpretations of the data.

Author Information Reprints and permissions information is available at www.nature.com/reprints. The authors declare no competing financial interests. Readers are welcome to comment on the online version of this article at www.nature.com/nature. Correspondence and requests for materials should be addressed to B.C.G. (bgill@fas.harvard.edu).